Controlling the mesostructure formation within the shell of novel cubic/hexagonal phase cetyltrimethylammonium bromide–poly(acrylamide-acrylic acid) capsules for pH stimulated release

Kristian J. Tangso,[a] Hetika Patel, [b] Seth Lindberg, [c] Patrick G. Hartley,[d] Robert Knott,[e] Patrick Spicer,[f] Ben J. Boyd[a,*]

*Email: ben.boyd@monash.edu

* To whom correspondence should be addressed. Email: ben.boyd@monash.edu

[a] Drug Delivery, Disposition and Dynamics and ARC Centre of Excellence in Convergent Bio-Nano Science and Technology, Monash Institute of Pharmaceutical Sciences, Monash University (Parkville Campus), 381 Royal Parade, Parkville, Victoria 3052, Australia

[b] University College London School of Pharmacy, 29-39 Brunswick Square, London WC1N 1AX, United Kingdom

[c] The Procter and Gamble Company, Corporate Engineering Technical Laboratories Building, Cincinnati, Ohio 45069, USA

[d] Commonwealth Scientific and Industrial Research Organization, Bag 10, Clayton South, VIC 3169, Australia

[e] Bragg Institute, Australian Nuclear Science and Technology Organization, Menai, NSW 2234, Australia

[f] School of Chemical Engineering, University of New South Wales, Sydney, NSW 2052, Australia

Abstract

The self-assembly of ordered structures in mixtures of oppositely charged surfactant and polymer systems has been exploited in various cleaning and pharmaceutical applications and continue to attract much interest since their discovery in the late twentieth century. The ability control the electrostatic and hydrophobic interactions that dictate the formation of liquid crystalline phases in these systems is advantageous in manipulation of structure and rendering them responsive to external stimuli. Nanostructured capsules comprised of the cationic surfactant, cetyltrimethylammonium bromide (CTAB), and the diblock copolymer poly(acrylamide-acrylic acid) (PAAm-AA) were prepared to assess their potential as pH responsive nanomaterials. Crossed-polarizing light microscopy (CPLM) and small angle X-ray scattering (SAXS) identified coexisting *Pm3n* cubic and hexagonal phases at the surfactant–polymer interface. The hydrophobic and electrostatic interactions between the oppositely charged components were studied by varying temperature and solution pH, respectively, and were found to influence the liquid crystalline nanostructure formed. The lattice parameter of the mesophases and the fraction of cubic phase in the system decreased upon heating. Acidic conditions resulted in the loss of the highly ordered structures due to protonation of the carboxylic acid group, and subsequent reduction of attractive forces previously present between the oppositely charged molecules. The rate of release of the model hydrophilic drug, Rhodamine B (RhB), from nanostructured macro-sized capsules significantly increased when the pH of the solution was adjusted from pH 7 to pH 2. This allowed for immediate release of the compound of interest 'on demand', opening new options for structured materials with increased functionality over typical layer-by-layer capsules.

KEYWORDS

poly(acrylamide-acrylic acid), cetyltrimethylammonium bromide, pH responsive, *Pm3n* cubic phase, hexagonal phase, release studies

1. Introduction

Since the emergence of self-assembled ordered structures in mixtures of oppositely charged surfactant and polymer systems four decades ago,[1-2] they continue to receive great attention especially targeted in cleaning, personal care, pharmaceutical and biomedical applications. The ability to attain control over the electrostatic and hydrophobic interactions that dictate the formation of liquid crystalline phases in these systems is advantageous in manipulation of structure and rendering them responsive to external stimuli. Variables that have impacted on the phase behavior, stability and/or size of nanostructures formed in these systems include temperature,[3-7] salt concentration[8-13] and pH.[14] The system consisting of the industrially relevant anionic surfactant, sodium dodecyl sulphate, and the cationic polymer, polydiallyldimethylammonium chloride, has been shown to form hexagonal phase-structured capsules, while the biorelevant anionic bile salt, sodium taurodeoxycholate, and the cationic polymer, chitosan, formed lamellar mesophase within the capsule shell.[15] These two systems were salt and temperature responsive respectively, releasing an encapsulated model hydrophilic drug 'on demand'.

The identification of similar nanostructured materials that are pH responsive is of particular interest as a variety of physiological states involve changes in pH, and consequently could be used in biomedical applications to act as a trigger for the release of active components from surfactant–polymer complexes.[16-17] In order for a material to be responsive to changes in pH it must possess a functional group that is susceptible to ionization. Poly(acrylic acid), poly(*N*,*N*-dimethylaminoethyl methacrylate), alginate and hyaluronic acid are examples of synthetic and natural polyelectrolytes that fall under this category.[18] They are commonly utilized as hydrogels, where differences in their swelling behavior at varying pH may be exploited as a means of stimulating the delivery of therapeutics. Mahdavinia *et al.* reported on how pH and salt influenced the swelling capacity of cross-linked hydrogels comprised of poly(acrylamide-acrylic acid) grafted with chitosan. Findings presented pH-dependent reversible swelling between pH 3 ("on") and pH 10 ("off") and that its swelling capacity was controlled by the

degree of cross-linking. The valency of the salt also affected the swelling capacity, where the presence of a divalent ion increased the cross-linking density by having a double interaction with the negatively charged functional group on the polymer, which led to the deswelling of the gel.[19] While interesting, these materials do not form nanostructured elements as is often found in oppositely charged surfactant–polymer systems.

Nizri *et al.* demonstrated that highly ordered nanostructures, namely hexagonal phase, can arise upon interaction between polyacrylate and alkyltrimethylammonium salts with a surfactant chain greater than eight carbons in length.[20] Cross-linking of polyacrylate produced macrogels which when in contact with a solution of CTAB resulted in its deswelling. This was explained by the diffusion of micelles into the stagnant macrogel and the subsequent formation of *Pm3n* cubic phase onto its surface, which transformed into hexagonal phase over time.[21] Hierarchical complex columnar phases have also been encountered when combining polyelectrolytic block copolymers with oppositely charged surfactants.[22]

In the study presented here, the formation of mesophases at the interface between solutions of the cationic surfactant, cetyltrimethylammonium bromide (CTAB), and the block copolymer, poly(acrylamide-acrylic acid) (PAAm-AA) (chemical structures shown in Figure 1), was investigated. It was hypothesized that the liquid crystalline phase(s) formed at the surfactant–polymer interface can be controlled by adjusting the solution pH, which in turn can modify the rate of release of a model hydrophilic drug from nanostructured capsules.

Specifically, the aims were to (a) identify the liquid crystalline phases formed at the interface between surfactant and polymer solutions, (b) study the growth and development of nanostructures across this interface, (c) probe the strength of hydrophobic and electrostatic interactions between moieties by examining how the nanostructures are influenced by changes in solution temperature and pH, and (d) determine the release behavior of incorporated model drug from macro-sized capsules possessing nanostructured ‘shells’ under different solution conditions.

2. Experimental section

2.1 Materials

The block copolymer poly(acrylamide-acrylic acid, sodium salt) (PAAm-AA, 40% carboxy, MW: > 10,000,000) was purchased from Polysciences Inc. (1-Hexadecyl)trimethyl-ammonium bromide, 98% (CTAB) was obtained from Alfa Aesar (UK). Rhodamine B (RhB, dye content ~90%) was sourced from Sigma-Aldrich (AUS). Sodium hydroxide pellets (Univar) were purchased from Ajax Chemicals (AUS) and hydrochloric acid (32% concentrated, Univol) was acquired from Asia Pacific Specialty Chemicals Limited (AUS). These materials were used as received. Milli-Q grade water, purified through a Milli-pore system was used throughout these experiments.

2.2 Characterization of liquid crystalline nanostructures

2.2.1 Sample preparation

Leonard *et al*. showed the existence of *Pm3n* cubic phase in mixtures of PAAm-AA and cetyltrimethylammonium chloride at charge stoichiometric amount, where the concentration of the polymer (40% carboxylate content) was fixed at 1 wt%.[23] In order to favour the formation of liquid crystalline structure(s) in the system of interest, the polymer, PAAm-AA, was also prepared at 1 wt % in Milli-Q water. The concentration of CTAB required to ensure that stoichiometric charge equivalence was achieved was calculated to be 2.5 wt%. Hence, all studies were performed at this composition. Aqueous solutions prepared for investigation were adjusted to either pH 7 or 2 by drop-wise addition of 0.1M NaOH or 32% concentrated HCl as required.

The kinetics of structure formation and phase behaviour at the interface between surfactant and polymer aqueous solutions was studied as described previously for other oppositely charged surfactant–polymer systems.[15] Briefly, PAAm-AA solution was drawn up from the bottom of an open-ended VitroCom glass ‘flat cell’ (dimensions: 0.4 x 8.0 x 50 mm, height x width x length) and sealed with parafilm. CTAB solution was then carefully pipetted into the top-end of the flat cell and the top sealed again with parafilm. This method allowed a neat interface to be created between the oppositely charged solutions of surfactant and polymer, which was marked as the ‘point of origin’ to enable temporal and

spatial resolution of the development of the interface. The internal dimension of the flat cell was 0.4 mm, which thereby determines the thickness of the same sample for microscopy and for SAXS studies.

A second configuration was also used to study the influence of pH on the mesophase(s) formed between solutions of CTAB and PAAm-AA, which allowed adjustment of the pH of the surrounding solution. Here, a circular interface was produced by delivering a disk of polymer solution inside the flat cell, which was subsequently flooded with CTAB solution to gain complete contact between the two components at pH 7. Structures were allowed to form at the interface over a defined time, after which the surrounding CTAB solution was replaced with Milli-Q water at pH 2.

2.2.2 Crossed-polarizing light microscopy (CPLM)

Crossed-polarized light microscopy was used to visualize the appearance of any anisotropic liquid crystalline structures formed at CTAB–PAAm-AA interfaces by detection of birefringence. Images were taken using a Nikon ECLIPSE Ni-U upright microscope fitted with crossed-polarizing filters and a DS-U3 digital camera control unit (Nikon, Japan) before and after changing the solution pH from 7 to 2.

2.2.3 Small angle X-ray scattering (SAXS)

Two different SAXS instruments were used to (1) spatially resolve the structures present at CTAB–PAAm-AA interfaces, and (2) to determine equilibrium phase behavior of mixtures with increasing temperature; both previously described by Tangso *et al.*[15] For spatial resolution of structure at interfaces, samples prepared in flat cells were mounted in the beam on a remotely operated XYZ translation stage at the SAXS beamline at the Australian Synchrotron.[24] A beam energy of 11 keV (wavelength of 1.1271 Å) and sample to detector distance of 1531.89 mm provided a q-range of 0.0103–0.5776 Å. An automated 'line scan' was conducted which involved rastering across the interface from the bulk polymer to surfactant solution at 100 μm steps (beam size: 200 x 100 μm, horizontal x vertical), acquiring SAXS 2D patterns for 1 s at each position using a 1M Pilatus detector (active area 169 x 179 mm^2 with a pixel size of 172 μm). The ScatterBrain Analysis in-house software was used to

reduce the 2D scattering patterns to the 1D scattering function I (q). The d-spacing of the liquid crystalline lattice is derived from Bragg's law ($\boldsymbol{2dsin\theta = n\lambda}$, where n is an integer, λ is the wavelength, θ is the scattering angle). SAXS scattering curves provide a characteristic fingerprint that allows the recognition of specific liquid crystalline phases in the sample.[25]

For the equilibrium phase behavior experiments, a bench-top SAXS at the Bragg Institute at the Australian Nuclear Science and Technology Organisation was utilized to assess the stability of the structures formed in the CTAB–PAAm-AA system to changes in temperature. A bulk sample mixture was prepared by drop-wise addition of 2.5 wt% CTAB solution (500 µL) into a solution of 1 wt% PAAm-AA (500 µL), vortex mixed, then left to equilibrate on rollers in an incubator oven set at *ca.* 37 °C for at least 1 week prior to analysis. As justified earlier, this composition was studied as it was the theoretical amount required to achieve charge equivalence, which would favor the formation of a coacervate. The sample was packed into a quartz glass capillary (Capillary Tube Supplies Ltd, Germany) with a path length of 2.0 mm, sealed with wax and then inserted into a thermostatted metal heating block controlled by a Peltier system accurate to ± 0.1°C. The sample was introduced to the beamline of a Bruker Nanostar SAXS camera, with pinhole collimation for point focus geometry. The instrument source was a copper rotating anode (0.3 m filament) operating at 45 kV and 110 mA, fitted with cross-coupled Göbel mirrors, resulting in CuKα radiation wavelength 1.54 Å. The SAXS camera was a Hi-star 2D detector (effective pixel size 100 µm) which was located 650 mm from the sample to provide a q-range of 0.008-0.3910 $Å^{-1}$. Scattering patterns were collected over 30 min under vacuum to minimise air scatter. Samples were heated stepwise from 25 °C to 60 °C at 5 °C increments.

2.3 *In vitro* release studies

In vitro release studies were conducted in triplicate with the aim to determine the diffusivity of a model hydrophilic drug, Rhodamine B (RhB; chemical structure shown in Schematic 1) across the permeable nanostructure(s) formed at interfaces between solutions of CTAB and PAAm-AA, and assess how the rate of drug release across the CTAB–PAAm-AA interface is influenced by changes in solution

pH. Macro-sized bead-like capsules possessing an ordered shell structure were prepared as previously described by introducing a droplet of one component into the other, as depicted in Schematic 1.[15, 26] A single droplet of PAAm-AA solution (1 wt%) containing 1 mg/mL RhB was delivered into a stirred solution of the release medium (1 mL in a 2 mL glass vial) via a 25 G needle, to form a nanostructured spherical capsule (~0.2 cm in diameter) with a reproducible surface area (~0.13 cm^2). The release medium was comprised of 2.5 wt% CTAB solution to initially form ordered structures at the surfactant–polymer interface and remained as the control system to avoid disruption of the capsule. The liquid crystalline structure present within the "shell" of the capsule was allowed to develop over time whilst submerged in the surfactant solution at pH 7 and maintained at *ca.* 37 °C. Aliquots (200 µL) of the release medium were sampled approximately every 5 min and replaced with 200 µL of fresh drug-free solution. To test the responsiveness of the system to pH, after ~30 min the surfactant solution was carefully removed, avoiding any disturbance to the capsule, then replenished with Milli-Q water adjusted to pH 2. Aliquots were further collected until ~100% of the dye was released from the capsules. The percentage of mass recovered was determined at the end of the study by comparing the initial mass of RhB loaded in the capsule with the mass of RhB measured in the release medium at the final time point.

2.3.1 Determination of Rhodamine B concentration in release medium

Aliquots of the release medium (CTAB solution) taken during the release study were diluted with Milli-Q water at their corresponding pH (either pH 7 or 2) and loaded into a 96 well plate. The fluorescence intensity of Rhodamine B in solution was measured at 37 °C using an EnSpire® Multimode Plate Reader (PerkinElmer, Singapore) with an excitation and emission wavelength of 554 nm and 627 nm, respectively. The concentration of dye released was quantified using a calibration curve of Rhodamine B in blank media at that pH (Figure S.1).

2.3.2 *In vitro* release data analysis

Calculation of the apparent diffusion coefficient, D (cm^2/s), of Rhodamine B across the single-sided matrix was derived by using the slope of the linear curve attained when the moles of drug released per unit area, Q (mol/cm^2), was plotted against the square root of time, $t^{1/2}$ ($s^{1/2}$), and applying it to the Higuchi equation[1],[27]

$$Q = 2 \cdot C_0 \cdot \sqrt{\frac{D \cdot t}{\pi}} \qquad [1]$$

where C_0 is the initial concentration of drug in the capsule (mol/cm^3). As it is well known that liquid crystalline systems generally display diffusion-controlled release,[28-31] data were plotted as % RhB released versus $time^{1/2}$.

3. Results

3.1 Liquid crystalline nanostructure formed across CTAB–PAAm-AA interfaces

3.1.1 Growth and development of nanostructure

Upon initial contact between the oppositely charged solutions of surfactant and polymer, the CTAB molecules already exists as micelles as indicated by the broad hump in the SAXS profile, whilst the PAAm-AA molecules displayed weak scattering (Figure 2-left). Highly ordered structures that spanned ~ 2 mm across the interface were identified as coexisting *Pm3n* cubic (√2:√4:√5:√6…) and hexagonal (1:√3:√4…) phases by indexing the Bragg reflections present in the SAXS scattering curves acquired across the surfactant–polymer interface (see supporting information). It should be noted that synchrotron SAXS offers a high flux of X-rays and signal-to-noise ratio that enables acquisition of highly resolved scattering profiles that is superior in comparison with what is obtained from a bench-top instrument. This is emphasized in the appearance of the Bragg peak at √2 for *Pm3n* cubic phases when characterized by synchrotron SAXS (Figure S2 and S3). However, it was unresolved in SAXS profiles obtained during the temperature scan with a bench-top SAXS instrument (Table S1 and S2, Figure S4).

These self-assembled mesophases grew predominantly towards the bulk CTAB micellar solution after 1 week (Figure 2).

Further examination of the structures formed at the interface showed distinct spatial trends in the lattice dimensions of the structures across the interface (Figure 2-right). Notably, the lattice parameter of the *Pm3n* cubic phase followed a somewhat sigmoidal curve, where the minimum lay near the bulk polymer region indicating the position of least swelling of the cubic structure, whereas the maximum was situated towards the bulk micellar region. Interestingly, the point of inflection in the change in lattice parameter for the cubic phase corresponded to the position across the interface where a significant drop in the internal dimensions of the hexagonal phase was observed, however the point of minimal swelling of the two phases was not spatially coincident.

3.1.2 Effect of temperature and pH on nanostructures

Following the identification of the structures that arise within the CTAB/PAAm-AA system, their equilibrium phase behavior and structural stability against changes to temperature and solution pH were then assessed. The coexisting *Pm3n* cubic and hexagonal phases persisted throughout heating of the bulk aqueous mixture of CTAB and PAAm-AA (Figure 3A) from 25 to 60 °C although the ratio between them changed (see Table S1 and Table S2 in supporting information for how the mesophases were indexed). As the temperature was increased, a number of the Bragg reflections indexed as *Pm3n* cubic phase gradually disappeared giving rise to a system being comprised majority of hexagonal phase. In addition, the Bragg peaks shifted towards higher q values upon heating, which correlated to a linear decrease in the lattice parameter with increasing temperature (Figure 3B).

In contrast to the weak dependence on temperature, the liquid crystalline phases that arise at the CTAB–PAAm-AA interface were strongly susceptible to pH. Reduction of the surrounding solution pH to 2 resulted in the disappearance of the Bragg reflections that were previously present in the SAXS scattering profile at pH 7 (Figure 4). This effect was also observed in the images taken under cross-

polarizers in which the band at the interface exhibiting birefringence vanished upon lowering of the solution pH (Figure 4- insets).

3.2 *In vitro* release studies

After establishing that the nanostructures formed at the CTAB–PAAm-AA interface were pH-sensitive, the diffusion of model drug (Rhodamine B) from macro-sized capsules was then studied. The *in vitro* release studies were conducted in the same format as previous studies at 37 ºC to enable direct comparison between the diffusion coefficient of Rhodamine B from other oppositely charged surfactant and polymer systems previously investigated by Tangso *et al*.[15] As depicted in Figure 5, the percentage of dye molecules released from the structured capsules increased linearly as a function of square root of time with a calculated diffusion coefficient of 0.087 ± 0.013 x10^{-6} cm^2s^{-1}. At approximately 44 $s^{1/2}$ (~32 min after the capsules were initially formed, highlighted by the position of the dashed arrow in Figure 5, the pH of the release medium was adjusted from pH 7 to 2. The pH shift resulted in a significant increase in the gradient of the release curve, reaching complete release within 5 min of the pH switch.

4. Discussion

4.1 Formation of cubic and hexagonal phases at the CTAB–PAAm-AA interface

The appearance of coexisting *Pm3n* cubic and hexagonal phases in CTAB–PAAm-AA complexes has been previously identified using small angle X-ray scattering,[23, 32-33] however their formation at liquid-liquid interfaces has not yet been reported until now. Inspection of the CTAB/water binary phase diagram by crossed-polarized light microscopy illustrates phase transitions between an isotropic phase to a viscous isotropic phase to a nematic phase and finally a hexagonal phase with increasing CTAB concentration.[34] While analysis by X-ray diffraction showed phase transitions between micellar → hexagonal → *Ia3d* cubic → lamellar phases with increasing surfactant concentration.[35] Since micelles were already present in the CTAB solution prepared at 2.5 wt% (~69 mM), a concentration that is well above its critical micellar concentration (cmc ≈ 0.9 mM measured by

steady-state fluorescence[36], 0.8 – 0.92 mM by surface tension measurements[37-38]), interaction with the solution of charged block copolymer resulted in the self-assembly of highly ordered structures at the neat interface created between the two components (Figure 2). Unlike the systems presented by Berret *et al.* and Uchman *et al.* which showed the formation of *Pm3n* cubic phase colloidal complexes with a core-shell microstructure (where the core was comprised of densely packed micelles and the shell containing the neutral polymeric chains) in aqueous mixtures of dodecyltrimethylammonium bromide and poly(sodium acrylate), and N-dodecylpyridinium chloride and poly(ethylene oxide)-block-poly(methacrylate), respectively, coexisting *Pm3n* cubic and hexagonal phases were found at the CTAB–PAAm-AA interface (Figure 2).[39-40] The *Pm3n* cubic phase has been described to be a construct of disconnected micellar aggregates composed of two types of elongated micelles packed in the unit cell,[33, 41] while the hexagonal phase is defined as cylindrical micelles arranged in a hexagonal lattice. Interestingly, the mesophases that spanned across the CTAB–PAAm-AA interface displayed differing lattice parameters ranging between 105–123 Å for *Pm3n* cubic phases and 50–58 Å for hexagonal phases. Smaller lattice parameters exhibited by the structures formed at the interface could possibly be explained by a higher concentration of the polymer that is locally present where it can act as a 'glue' and assist in the compression of ordered structures.

The scattering indicates the presence of hexagonal and cubic phases. There are two descriptions of the situation, (i) that the two phases are coexisting in equilibrium, which is supported by the fact that their proportion changes during the equilibrium temperature ramp study, or (ii) that there is nonequilibrium trapping of one or both of the structures at the interface. The latter case might reasonably be expected to produce bands of structure with and without birefringence in the microscopy studies, which was evident. Nevertheless, nonequilibrium structures are often kinetically trapped in these systems depending on the method of preparation.[11, 42-46] It is also known that mixing is not an instantaneous process, especially when studying the system at high surfactant and polymer concentrations where the inherent viscosity of each solution influences the ability of the molecules to diffuse into the other component to form structures at equilibrium.[47] However, the evidence in this study

indicates that coexisting cubic and hexagonal phases at or close to equilibrium are more likely in this case.

Another intriguing facet to the phase behavior at the CTAB–PAAm-AA interface studied here was its development predominantly towards the bulk micellar region. As the coexisting cubic and hexagonal phases are postulated to be highly viscous, this introduces a barrier that molecules will have to traverse to further interact with free or bound micellar structures. The most probable reason behind this outcome would be the movement of water molecules from the bulk polymer solution which in turn drives the transportation of more PAAm-AA molecules through the permeable interface and form interactions with the existing maze of complexes. A better understanding of the kinetics of structure formation at surfactant–polymer interfaces may be attained by correlating changes in structure with changes in composition as a function of time. An approach to address this is currently being developed.

4.2 Structural responsiveness of the cubic/hexagonal phases in CTAB–PAAm-AA systems

A wide variety of lyotropic lipid based liquid crystalline systems have demonstrated structural responsiveness to various stimuli such as, ultraviolet or near-infrared irradiation through activation of photochromic additives,[48-49] changes in solution pH,[50-51] and temperature,[28] all of which alter the geometric packing within the mesophase, resulting in a different phase structure. Similarly, structures formed in oppositely charged surfactant and polymer systems can be tuned by studying parameters that influence the electrostatic and hydrophobic interactions that govern their self-assembly in water.

A temperature scan on a bulk aqueous mixture of CTAB and PAAm-AA was conducted to probe the hydrophobic interactions between the surfactant and polymer molecules. SAXS data showed that the coexisting cubic and hexagonal phases were sensitive to increasing temperatures, but was not sufficient to cause a full phase transition. This implies that heating of the sample slightly weakens the hydrophobic interactions, thus stimulating mobility within the liquid crystalline structure. This gives the molecules more freedom to re-orientate themselves and pack more tightly in an ordered structure as seen by a decrease in lattice parameter. It is also worth mentioning that the hexagonal phase dominated

in existence with minimal *Pm3n* cubic phase present at the highest temperature experienced by the system. This phase behavior was more prominent when the effect of osmotic pressure on the compressibility of the mesophases formed in a similar system was measured. The following phase transitions were reported with increasing osmotic pressure: *Pm3n* cubic phase (100–150 Å) → hexagonally closed-packed cylinders (45–60 Å) → lamellar phase (25–35 Å), where a decrease in lattice parameter of the structures was also observed with an increase in charge density of the di-block copolymer.[23] Nilsson *et al*. also demonstrated a *Pm3n* cubic to hexagonal phase transition at the interface between a polyacrylate gel and a solution of CTAB.[21] As more surfactant molecules diffused into the core of the gel, the concentration of the bromide ions increased, which promoted the formation of a more condensed structure, namely hexagonal phase. Therefore, heat can evidently be employed to drive the phase behavior of the system presented in this paper in the expected direction, from coexisting *Pm3n* cubic and hexagonal phases to hexagonal phase which constitutes structure that is at equilibrium.

On the other hand, exposing the CTAB–PAAm-AA interface to an acidic environment led to the complete loss of the nanostructures which had formed there at neutral pH. At pH 7, the carboxylic acid group (pKa ~ 5.4)[52] on the polymer backbone is deprotonated giving it a negative net charge. Ionization of this functional group promotes its interaction with the positively charged surfactant and the subsequent release of the counterions that causes an increase in entropy of the system both contributing to the spontaneous formation of the coexisting cubic and hexagonal phases at the surfactant–polymer interface. At pH 2, the opposite effect occurs, where the acrylic acid portion of the polymer becomes protonated, thus losing its negative charge. This, along with a fraction of the acrylamide (pKa ~2.45) monomer units attaining a positive charge introduces a repulsive force that exceeds the hydrophobic interactions involved in maintaining its structural integrity lead to the dissociation of the highly ordered structures. The effect of pH on the ionization state of functional groups on the polymer chain was much subtler in the system comprised of poly(vinylamine) and sodium alkyl sulfates. Zhou *et al.* demonstrated phase transitions from a two-dimensional distorted hexagonal phase at pH 5.8, to a lamellar phase at pH 8.9 and a two-dimensional hexagonal close packed phase at pH 12.2. This signifies the importance of

the charge density exhibited by the polymer at varying pH, which is dictated by its pKa, in tuning the structure of the complex formed.[53]

4.3 pH triggered release of model drug from CTAB–PAAm-AA cubic/hexagonal capsules

The release of active agents from capsules formed from associations between solutions of oppositely charged surfactant and polymer systems can be controlled by structural changes.[47, 54-55] Here, the diffusivity of the model hydrophilic drug, Rhodamine B, from capsules possessing differing geometries, studied under the same conditions, can be compared. The hierarchy of the diffusion coefficients calculated for the *in vitro* release studies performed on various oppositely charged surfactant–polymer systems conducted at 37 ºC are as follows: a > b >>> c. The release behavior exhibited from (a) coexisting cubic *Pm3n* and hexagonal phases formed at the interface created between solutions of CTAB and PAAm-AA described in this paper, (b) lamellar phase formed at the interface between bile salt and chitosan, and (c) hexagonal phase formed at the interface between sodium dodecyl sulphate and poly(diallyldimethylammonium) chloride demonstrates that the interactions that govern the nanostructures formed play a notable bearing on their inherent physical properties, such as their viscosity, which subsequently controls the permeability of molecules through the intricate matrices. More specifically, the differences in the lattice parameter of the ordered structures partly support the distinct release behavior demonstrated from the various nanostructured capsules. Since the lattice parameter gives a numerical indication of the internal structure, or rather the internal dimensions of the liquid crystalline phase, smaller values which are characteristic of hexagonal phases would lead to a more compacted network of molecules through which drug molecules will have to diffuse and consequently the time it would take for it to be released would also increase. Conversely, the rate of drug release is faster with the coexistence of *Pm3n* cubic phase with hexagonal phase in the PAAm-AA–CTAB system. This is a result of the lattice parameter of the cubic phase being more than double in size in comparison with the hexagonal phase alone, which also suggests that the cubic phase is the dominating structure that exists in this system and therefore is the key determinant of the release

behavior observed. Moreover, lamellar phase is known to be quite a leaky structure and so it is not surprising that the diffusion coefficient for Rhodamine B from the bile salt–chitosan system was found to be in between the other two oppositely charged surfactant and polymer systems.

pH is often a desirable means of imparting responsiveness to liquid crystalline structures by changing the extent of ionization state of a particular component of a drug carrier system. Directly linking the *in situ* formation (and loss) of structure in these systems with changes in pH, and consequently demonstrating release of an encapsulated molecule is new for systems comprised of CTAB and PAAm-AA. This behavior can be used to take advantage of changes in cellular pH[56], for example in tumors,[51, 57] or even the range of pH the gastrointestinal tract[58].

Of particular interest is the exploitation of hyaluronic acid, which is a naturally occurring polysaccharide involved in, but not limited to, the maintenance of connective tissues in living organisms.[59] Its biodegradability, biocompatibility and low toxicity is advantageous in the field of targeted drug delivery, where the carboxyl group functions as a ligand to hyaluronan CD-44 receptors that are overexpressed in solid tumour cells.[60] When conjugated with the anticancer drug, paclitaxel, nanoparticles coated with chitosan to protect it from degradation by hyaluronidase, were found to accumulate in tumours cells via cell-mediated endocytosis, providing a platform for oral delivery of hydrophobic drugs.[61] Furthermore, when hyaluronic acid was conjugated with poly(L-histidine), the ionisation of the imidazole ring of poly(L-histidine) in response to changes in solution pH was shown to dictate the swelling behaviour of the copolymer micelles and subsequent release of the encapsulated chemotherapeutic drug, doxorubicin.[62] In addition, hyaluronic acid has been blended with poloxamers to increase the stability and mechanical properties of gels formed *in situ* in response to physiological temperature.[63] Mayol *et al.* demonstrated that the ionisation of hyaluronic acid enhanced the mucoadhesion of the polaxomer, which in turn increased the residence time and bioavailability of the drug, acyclovir. Here, temperature was used to control the viscosity of the formulation through changes in the degree of molecular entanglements and secondary chemical bonds within the poloxamer, offering a potential system for sustained-release ocular drug delivery.[63]

Cetyltrimethylammonium bromide and poly(acrylamide-acrylic acid) are not biocompatible and are considered unsuitable for the delivery of actives in the body. Nevertheless, this system serves as a confirmatory system for such behaviour providing confidence that analogous biocompatible oppositely charged surfactant and polymer systems will show similar pH responsive behavior. The use of these materials is not excluded in external applications either such as fragrance release, or in sensing and diagnostic applications where the materials could provide a highly controllable amplification function.

Future studies involving pH responsive biocompatible oppositely charged surfactant and polymer systems are underway.

5. Conclusion

This paper describes the coexistence of *Pm3n* cubic and hexagonal phases at the interface created between oppositely charged surfactant and polymer solutions of cetyltrimethylammonium bromide and poly(acrylamide-acrylic acid), respectively. These highly ordered liquid crystalline nonequilibrium structures were found to be weakly sensitive to increases in temperature, but dramatically sensitive to changes in solution pH. *In vitro* release studies demonstrated the pH triggered release of model hydrophilic dye from nanostructured capsules, which serves as a platform for devising systems that are responsive to changes in solution pH, particularly in the application of biomaterials.

Acknowledgments.

The authors acknowledge the Australian Institute of Nuclear Science and Engineering (ALNGRA11161), Procter & Gamble, and the Commonwealth Scientific and Industrial Research Organization (CSIRO) for funding this project. K.J.T also thanks AINSE for support in the form of a Postgraduate Graduate Research Award. SAXS studies were conducted on the SAXS/WAXS beamline at the Australian Synchrotron, Victoria, Australia, as well as at the Bragg Institute at ANSTO. BB is the recipient of an ARC Future Fellowship.

Supporting Information Available.

The calibration curve for Rhodamine B in Milli-Q water prepared at pH 7 and 2, and a summary of how the coexisting mesophases were indexed are available free of charge via the Internet at http//pubs.acs.org/.

References

1. Goddard, E. D.; Hannan, R. B., Cationic Polymer/Anionic Surfactant Interactions. *J Colloid Interface Sci* **1976,** *55*, 73-79.

2. Goddard, E.; Hannan, R., Polymer/Surfactant Interactions. *J Am Oil Chem Soc* **1977,** *54*, 561-566.

3. Sokolov, E.; Yeh, F.; Khokhlov, A.; Grinberg, V. Y.; Chu, B., Nanostructure Formation in Polyelectrolyte−Surfactant Complexes. *J Phys Chem B* **1998,** *102*, 7091-7098.

4. Merta, J.; Torkkeli, M.; Ikonen, T.; Serimaa, R.; Stenius, P., Structure of Cationic Starch (Cs)/Anionic Surfactant Complexes Studied by Small-Angle X-Ray Scattering (Saxs). *Macromolecules* **2001,** *34*, 2937-2946.

5. Bilalov, A.; Olsson, U.; Lindman, B., DNA-Lipid Self-Assembly: Phase Behavior and Phase Structures of a DNA-Surfactant Complex Mixed with Lecithin and Water. *Soft Matter* **2011,** *7*, 730-742.

6. Rondon, C.; Argillier, J.-F.; Leal-Calderon, F., Delivery of Functional Polyelectrolytes from Complexes Induced by Salt Addition: Impact of the Initial Binding Strength. *J Colloid Interface Sci* **2014,** *436*, 154-159.

7. Hsu, W.-L.; Li, Y.-C.; Chen, H.-L.; Liou, W.; Jeng, U. S.; Lin, H.-K.; Liu, W.-L.; Hsu, C.-S., Thermally-Induced Order−Order Transition of DNA−Cationic Surfactant Complexes. *Langmuir* **2006,** *22*, 7521-7527.

8. Abraham, A.; Mezei, A.; Meszaros, R., The Effect of Salt on the Association between Linear Cationic Polyelectrolytes and Sodium Dodecyl Sulfate. *Soft Matter* **2009,** *5*, 3718-3726.

9. Mezei, A. l.; Ábrahám, A. g.; Pojják, K.; Mészáros, R. b., The Impact of Electrolyte on the Aggregation of the Complexes of Hyperbranched Poly(Ethyleneimine) and Sodium Dodecyl Sulfate. *Langmuir* **2009,** *25*, 7304-7312.

10. Mironov, A. V.; Starodoubtsev, S. G.; Khokhlov, A. R.; Dembo, A. T.; Yakunin, A. N., Ordered Nonstoichiometric Polymer Gel−Surfactant Complexes in Aqueous Medium with High Ionic Strength. *Macromolecules* **1998,** *31*, 7698-7705.

11. Naderi, A.; Claesson, P. M.; Bergström, M.; Dėdinaitė, A., Trapped Non-Equilibrium States in Aqueous Solutions of Oppositely Charged Polyelectrolytes and Surfactants: Effects of Mixing Protocol and Salt Concentration. *Colloid Surface Physicochem Eng Aspect* **2005,** *253*, 83-93.

12. Bastardo, L. A.; Iruthayaraj, J.; Lundin, M.; Dedinaite, A.; Vareikis, A.; Makuška, R.; van der Wal, A.; Furó, I.; Garamus, V. M.; Claesson, P. M., Soluble Complexes in Aqueous Mixtures of Low Charge Density Comb Polyelectrolyte and Oppositely Charged Surfactant Probed by Scattering and Nmr. *J Colloid Interface Sci* **2007,** *312*, 21-33.

13. Bera, T.; Deng, J.; Fang, J., Protein-Induced Configuration Transitions of Polyelectrolyte-Modified Liquid Crystal Droplets. *J Phys Chem B* **2014**.

14. Chiappisi, L.; Prévost, S.; Grillo, I.; Gradzielski, M., Chitosan/Alkylethoxy Carboxylates: A Surprising Variety of Structures. *Langmuir* **2014,** *30*, 1778-1787.

15. Tangso, K. J.; Lindberg, S.; Hartley, P. G.; Knott, R.; Spicer, P.; Boyd, B. J., Formation of Liquid-Crystalline Structures in the Bile Salt–Chitosan System and Triggered Release from Lamellar Phase Bile Salt–Chitosan Capsules. *ACS Appl Mater Interfaces* **2014,** *6*, 12363-12371.

16. Negrini, R.; Mezzenga, R., Ph-Responsive Lyotropic Liquid Crystals for Controlled Drug Delivery. *Langmuir* **2011,** *27*, 5296-5303.

17. Rahanyan-Kägi, N.; Aleandri, S.; Speziale, C.; Mezzenga, R.; Landau, E. M., Stimuli-Responsive Lipidic Cubic Phase: Triggered Release and Sequestration of Guest Molecules. *Chem Eur J* **2015,** *21*, 1873-1877.

18. Dai, S.; Ravi, P.; Tam, K. C., Ph-Responsive Polymers: Synthesis, Properties and Applications. *Soft Matter* **2008,** *4*, 435-449.

19. Mahdavinia, G. R.; Pourjavadi, A.; Hosseinzadeh, H.; Zohuriaan, M. J., Modified Chitosan 4. Superabsorbent Hydrogels from Poly(Acrylic Acid-Co-Acrylamide) Grafted Chitosan with Salt- and Ph-Responsiveness Properties. *Eur Polymer J* **2004,** *40*, 1399-1407.

20. Nizri, G.; Makarsky, A.; Magdassi, S.; Talmon, Y., Nanostructures Formed by Self-Assembly of Negatively Charged Polymer and Cationic Surfactants. *Langmuir* **2009,** *25*, 1980-1985.

21. Nilsson, P.; Hansson, P., Regular and Irregular Deswelling of Polyacrylate and Hyaluronate Gels Induced by Oppositely Charged Surfactants. *J Colloid Interface Sci* **2008,** *325*, 316-323.

22. Li, C.; Schluüter, A. D.; Zhang, A.; Mezzenga, R., A New Level of Hierarchical Structure Control by Use of Supramolecular Self-Assembled Dendronized Block Copolymers. *Adv Mater* **2008,** *20*, 4530-4534.

23. Leonard, M. J.; Strey, H. H., Phase Diagrams of Stoichiometric Polyelectrolyte−Surfactant Complexes. *Macromolecules* **2003,** *36*, 9549-9558.

24. Kirby, N. M.; Mudie, S. T.; Hawley, A. M.; Cookson, D. J.; Mertens, H. D. T.; Cowieson, N.; Samardzic-Boban, V., A Low-Background-Intensity Focusing Small-Angle X-Ray Scattering Undulator Beamline. *J Appl Crystallogr* **2013,** *46*, 1670-1680.

25. Hyde, S., Chapter 16- Identification of Lyotropic Liquid Crystalline Mesophases. In *Handbook of Applied Surface and Colloid Chemistry*, Holmberg, K., Ed. John Wiley & Sons, Ltd: **2001** pp 299-332.

26. Babak, V. G.; Merkovich, E. A.; Desbrières, J.; Rinaudo, M., Formation of an Ordered Nanostructure in Surfactant-Polyelectrolyte Complexes Formed by Interfacial Diffusion. *Polymer Bull* **2000,** *45*, 77-81.

27. Higuchi, W. I., Diffusional Models Useful in Biopharmaceutics. Drug Release Rate Processes. *J Pharmaceut Sci* **1967,** *56*, 315-324.

28. Fong, W.-K.; Hanley, T.; Boyd, B. J., Stimuli Responsive Liquid Crystals Provide 'on-Demand' Drug Delivery *in Vitro* and *in Vivo*. *J Contr Release* **2009,** *135*, 218-226.

29. Lee, K. W. Y.; Nguyen, T.-H.; Hanley, T.; Boyd, B. J., Nanostructure of Liquid Crystalline Matrix Determines in Vitro Sustained Release and in Vivo Oral Absorption Kinetics for Hydrophilic Model Drugs. *Int J Pharm* **2009,** *365*, 190-199.

30. Phan, S.; Fong, W.-K.; Kirby, N.; Hanley, T.; Boyd, B. J., Evaluating the Link between Self-Assembled Mesophase Structure and Drug Release. *Int J Pharm* **2011,** *421*, 176-182.

31. Zabara, A.; Negrini, R.; Baumann, P.; Onaca-Fischer, O.; Mezzenga, R., Reconstitution of Ompf Membrane Protein on Bended Lipid Bilayers: Perforated Hexagonal Mesophases. *ChemComm* **2014,** *50*, 2642-2645.

32. Leonard, M.; Hong, H.; Easwar, N.; Strey, H. H., Soft Matter under Osmotic Stress. *Polymer* **2001,** *42*, 5823-5827.

33. Leonard, M.; Strey, H. H., Measurement of Phase Transition Free Energies in Polyelectrolyte−Surfactant Complexes. *Macromolecules* **2010,** *43*, 4379-4383.

34. Hertel, G.; Hoffmann, H., Lyotropic Nematic Phases of Double Chain Surfactants. In *Trends in Colloid and Interface Science Ii*, Degiorgio, V., Ed. Steinkopff: **1988**; Chapter 23, pp 123-131.

35. Auvray, X.; Petipas, C.; Anthore, R.; Rico, I.; Lattes, A., X-Ray Diffraction Study of Mesophases of Cetyltrimethylammonium Bromide in Water, Formamide, and Glycerol. *J Phys Chem* **1989,** *93*, 7458-7464.

36. Li, W.; Zhang, M.; Zhang, J.; Han, Y., Self-Assembly of Cetyl Trimethylammonium Bromide in Ethanol-Water Mixtures. *Frontiers of Chemistry in China* **2006,** *1*, 438-442.

37. Gao, H.; Zhu, R.; Yang, X.; Mao, S.; Zhao, S.; Yu, J.; Du, Y., Properties of Polyethylene Glycol (23) Lauryl Ether with Cetyltrimethylammonium Bromide in Mixed Aqueous Solutions Studied by Self-Diffusion Coefficient Nmr. *J Colloid Interface Sci* **2004,** *273*, 626-631.

38. Hernáinz, F.; Caro, A., Variation of Surface Tension in Aqueous Solutions of Sodium Dodecyl Sulfate in the Flotation Bath. *Colloids Surf, A* **2002,** *196*, 19-24.

39. Berret, J.-F.; Vigolo, B.; Eng, R.; Hervé, P.; Grillo, I.; Yang, L., Electrostatic Self-Assembly of Oppositely Charged Copolymers and Surfactants: A Light, Neutron, and X-Ray Scattering Study. *Macromolecules* **2004,** *37*, 4922-4930.

40. Uchman, M.; Štěpánek, M.; Prévost, S.; Angelov, B.; Bednár, J.; Appavou, M.-S.; Gradzielski, M.; Procházka, K., Coassembly of Poly(Ethylene Oxide)-Block-Poly(Methacrylic Acid) and N-Dodecylpyridinium Chloride in Aqueous Solutions Leading to Ordered Micellar Assemblies within Copolymer Aggregates. *Macromolecules* **2012,** *45*, 6471-6480.

41. Fontell, K., Cubic Phases in Surfactant and Surfactant-Like Lipid Systems. *Colloid & Polymer Sci* **1990,** *268*, 264-285.

42. Pojják, K.; Bertalanits, E.; Mészáros, R., Effect of Salt on the Equilibrium and Nonequilibrium Features of Polyelectrolyte/Surfactant Association. *Langmuir* **2011,** *27*, 9139-9147.

43. Mezei, A. l.; Pojják, K.; Mészáros, R. b., Nonequilibrium Features of the Association between Poly(Vinylamine) and Sodium Dodecyl Sulfate: The Validity of the Colloid Dispersion Concept. *J Phys Chem B* **2008,** *112*, 9693-9699.

44. Fegyver, E.; Meszaros, R., Fine-Tuning the Nonequilibrium Behavior of Oppositely Charged Macromolecule/Surfactant Mixtures Via the Addition of Nonionic Amphiphiles. *Langmuir* **2014**.

45. Mezei, A.; Mészáros, R.; Varga, I.; Gilányi, T., Effect of Mixing on the Formation of Complexes of Hyperbranched Cationic Polyelectrolytes and Anionic Surfactants. *Langmuir* **2007,** *23*, 4237-4247.

46. Naderi, A.; Claesson, P. M., Association between Poly(Vinylamine) and Sodium Dodecyl Sulfate: Effects of Mixing Protocol, Blending Procedure, and Salt Concentration. *J Dispersion Sci Technol* **2005,** *26*, 329-340.

47. Lapitsky, Y.; Eskuchen, W. J.; Kaler, E. W., Surfactant and Polyelectrolyte Gel Particles That Swell Reversibly. *Langmuir* **2006,** *22*, 6375-6379.

48. Tangso, K. J.; Fong, W.-K.; Darwish, T.; Kirby, N.; Boyd, B. J.; Hanley, T. L., Novel Spiropyran Amphiphiles and Their Application as Light-Responsive Liquid Crystalline Components. *J Phys Chem B* **2013,** *117*, 10203-10210.

49. Fong, W.-K.; Hanley, T. L.; Thierry, B.; Kirby, N.; Waddington, L. J.; Boyd, B. J., Controlling the Nanostructure of Gold Nanorod–Lyotropic Liquid-Crystalline Hybrid Materials Using near-Infrared Laser Irradiation. *Langmuir* **2012,** *28*, 14450-14460.

50. Salentinig, S.; Tangso, K. J.; Hawley, A.; Boyd, B. J., Ph-Driven Colloidal Transformations Based on the Vasoactive Drug Nicergoline. *Langmuir* **2014**.

51. Negrini, R.; Fong, W.-K.; Boyd, B. J.; Mezzenga, R., Ph-Responsive Lyotropic Liquid Crystals and Their Potential Therapeutic Role in Cancer Treatment. *Chem Commun* **2015**.

52. Annaka, M., Salt Effect on Microscopic Structure and Stability of Colloidal Complex Obtained from Neutral/Polyelectrolyte Block Copolymer and Oppositely Charged Surfactant. *Colloids Surf, B* **2012,** *99*, 127-135.

53. Zhou, S.; Hu, H.; Burger, C.; Chu, B., Phase Structural Transitions of Polyelectrolyte−Surfactant Complexes between Poly(Vinylamine Hydrochloride) and Oppositely Charged Sodium Alkyl Sulfate. *Macromolecules* **2001,** *34*, 1772-1778.

54. Lapitsky, Y.; Kaler, E. W., Formation and Structural Control of Surfactant and Polyelectrolyte Gels. *Colloids Surf, A* **2006,** *282–283*, 118-128.

55. Lapitsky, Y.; Kaler, E. W., Formation of Surfactant and Polyelectrolyte Gel Particles in Aqueous Solutions. *Colloids Surf, A* **2004,** *250*, 179-187.

56. Yu, H.; Zou, Y.; Wang, Y.; Huang, X.; Huang, G.; Sumer, B. D.; Boothman, D. A.; Gao, J., Overcoming Endosomal Barrier by Amphotericin B-Loaded Dual Ph-Responsive Pdma-B-Pdpa Micelleplexes for Sirna Delivery. *ACS Nano* **2011,** *5*, 9246-9255.

57. Kim, B.-S.; Lee, H.-i.; Min, Y.; Poon, Z.; Hammond, P. T., Hydrogen-Bonded Multilayer of Ph-Responsive Polymeric Micelles with Tannic Acid for Surface Drug Delivery. *Chem Commun* **2009**, 4194-4196.

58. Salentinig, S.; Phan, S.; Darwish, T. A.; Kirby, N.; Boyd, B. J.; Gilbert, E. P., Ph-Responsive Micelles Based on Caprylic Acid. *Langmuir* **2014,** *30*, 7296-7303.

59. Liao, Y.-H.; Jones, S. A.; Forbes, B.; Martin, G. P.; Brown, M. B., Hyaluronan: Pharmaceutical Characterization and Drug Delivery. *Drug Delivery* **2005,** *12*, 327-342.

60. Mero, A.; Campisi, M., Hyaluronic Acid Bioconjugates for the Delivery of Bioactive Molecules. *Polymers* **2014,** *6*, 346.

61. Li, J.; Huang, P.; Chang, L.; Long, X.; Dong, A.; Liu, J.; Chu, L.; Hu, F.; Liu, J.; Deng, L., Tumor Targeting and Ph-Responsive Polyelectrolyte Complex Nanoparticles Based on Hyaluronic Acid-Paclitaxel Conjugates and Chitosan for Oral Delivery of Paclitaxel. *Macromol. Res.* **2013,** *21*, 1331-1337.

62. Qiu, L.; Li, Z.; Qiao, M.; Long, M.; Wang, M.; Zhang, X.; Tian, C.; Chen, D., Self-Assembled Ph-Responsive Hyaluronic Acid–G-Poly(L-Histidine) Copolymer Micelles for Targeted Intracellular Delivery of Doxorubicin. *Acta Biomaterialia* **2014,** *10*, 2024-2035.

63. Mayol, L.; Quaglia, F.; Borzacchiello, A.; Ambrosio, L.; Rotonda, M. I. L., A Novel Poloxamers/Hyaluronic Acid in Situ Forming Hydrogel for Drug Delivery: Rheological, Mucoadhesive and in Vitro Release Properties. *Eur J Pharm Biopharm* **2008,** *70*, 199-206.

Figure Captions

Figure 1. Chemical structures of the cationic surfactant, cetyltrimethylammonium bromide (CTAB), and the monomer units, acrylamide (AAm) and acrylic acid (AA), that comprise the polyelectrolyte, poly(acrylamide-acrylic acid) (PAAm-AA).

Figure 2. SAXS scattering profiles as a function of distance from origin, D, obtained during a spatial line scan across a system comprised of 2.5 wt% CTAB (top) and 1 wt% PAAm-AA solution (bottom). Coexisting cubic and hexagonal phase was shown to predominantly grow towards the bulk CTAB region after 1 week from initial contact between the two solutions (0 mm). This behavior and the differences in the lattice parameter of the *Pm3n* cubic (squares) and hexagonal (circles) phases formed at the

interface is mapped and highlighted on the right. See supporting information for q vs. intensity profiles at three pertinent representative D values (Figure S2).

Figure 3. Influence of temperature on the equilibrium phase behavior of coexisting cubic and hexagonal existing in a mixture comprised of 2.5 wt% CTAB and 1 wt% PAAm-AA. **A:** SAXS scattering profiles obtained for the system when heated from 25 to 60 °C at 5 °C increments. **B:** Changes in the lattice parameter (size) of coexisting *Pm3n* cubic (squares) and hexagonal (circles) phases in response to heating.

Figure 4. Effect of solution pH on the structural integrity of mesophase(s) formed at the CTAB–PAAm-AA interface**.** SAXS scattering profile shows the loss of coexisting cubic and hexagonal phase (left) after flushing the system with acidic solution (right). Insets: CPLM images.

Schematic 1. Illustration of the approach employed for studying the influence of solution pH on the rate of model drug (Rhodamine B, RhB) release from nanostructured capsules.

Figure 5. Cumulative % release profile of Rhodamine B (RhB) from structured CTAB–PAAm-AA capsules at *ca.* 37 °C (n=3). The dashed arrow indicates when the surfactant solution (pH 7) was replaced with Milli-Q water at pH 2; the point at which burst release of the dye was observed due to loss of structure at acidic conditions.

1
2

Figure 1

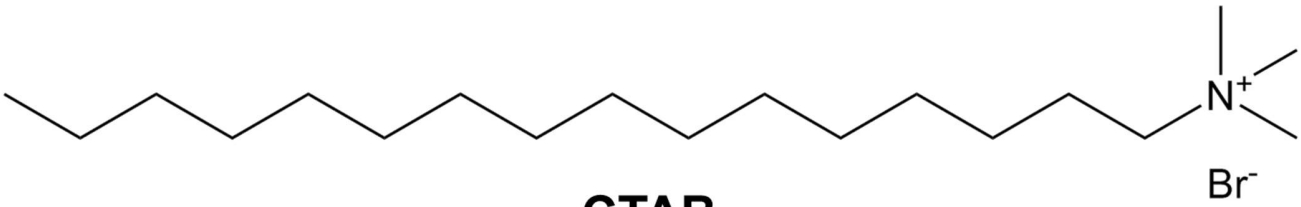

CTAB

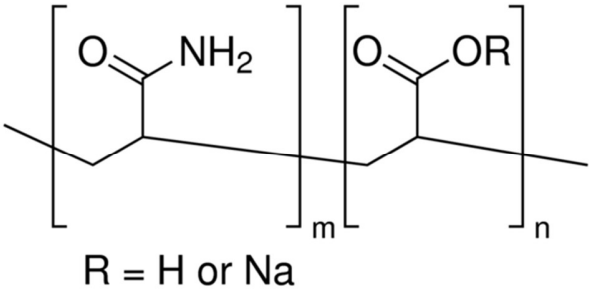

PAAm-AA

Figure 2

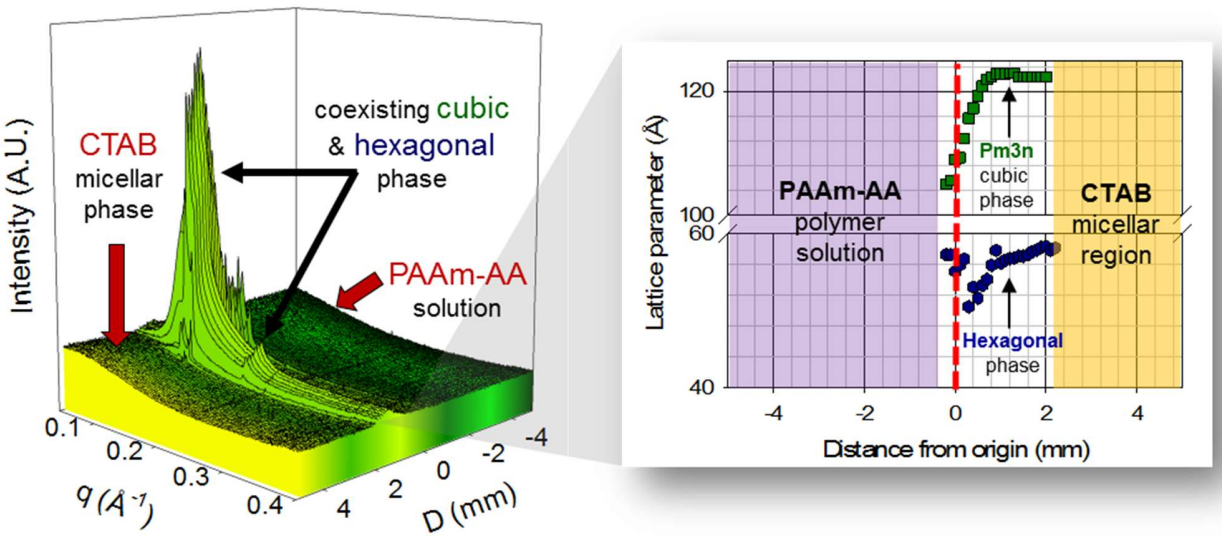
Intensity (A.U.)
CTAB
micellar
phase
coexisting cubic
& hexagonal
phase
PAAm-AA
solution
0.1
0.2
0.3
0.4
q (Å⁻¹)
4
2
0
-2
-4
D (mm)
Lattice parameter (Å)
120
100
60
40
PAAm-AA
polymer
solution
Pm3n
cubic
phase
CTAB
micellar
region
Hexagonal
phase
-4
-2
0
2
4
Distance from origin (mm)

Figure 3

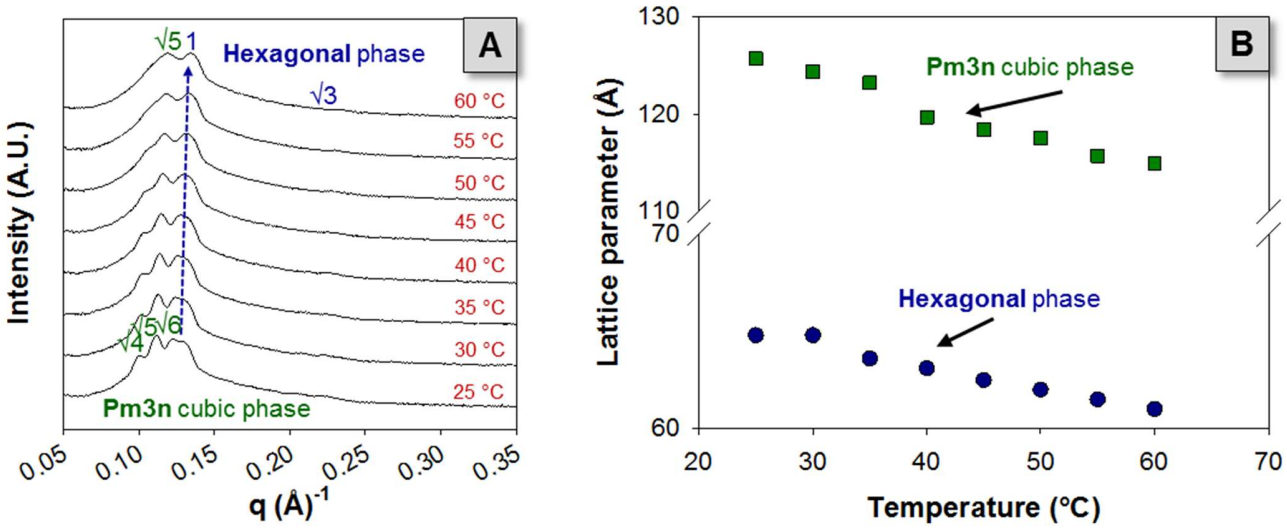
A
√5 1
Hexagonal phase
√3
60 °C
55 °C
50 °C
45 °C
40 °C
35 °C
30 °C
25 °C
√5√6
√4
Pm3n cubic phase
Intensity (A.U.)
0.05
0.10
0.15
0.20
0.25
0.30
0.35
q (Å)-1
B
Pm3n cubic phase
Hexagonal phase
Lattice parameter (Å)
130
120
110
70
60
20
30
40
50
60
70
Temperature (°C)

Figure 4

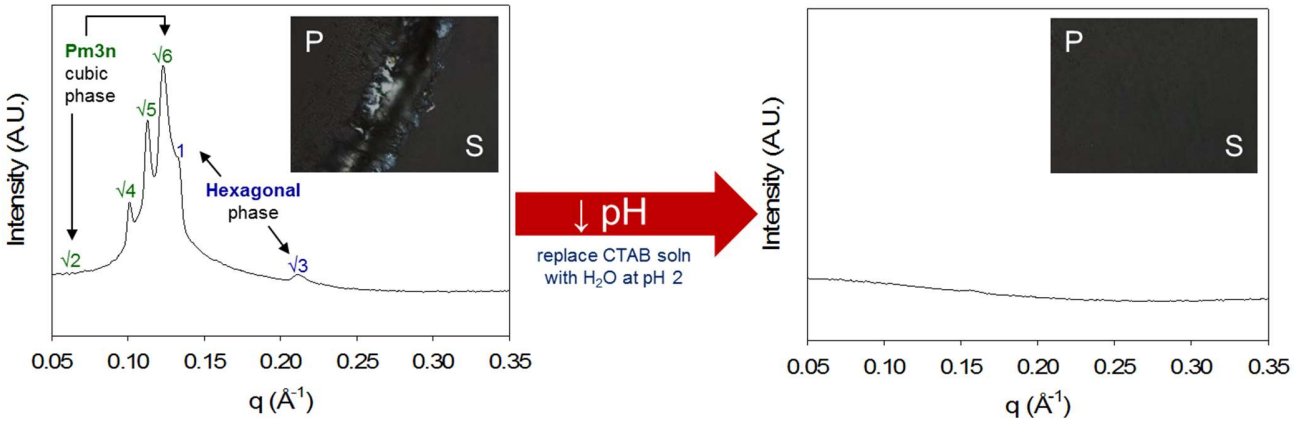
Pm3n
cubic
phase
√6
√5
1
√4
√2
√3
Hexagonal
phase
P
S
Intensity (A.U.)
0.05
0.10
0.15
0.20
0.25
0.30
0.35
q (Å-1)
↓ pH
replace CTAB soln
with H2O at pH 2
P
S
Intensity (A.U.)
0.05
0.10
0.15
0.20
0.25
0.30
0.35
q (Å-1)

Schematic 1

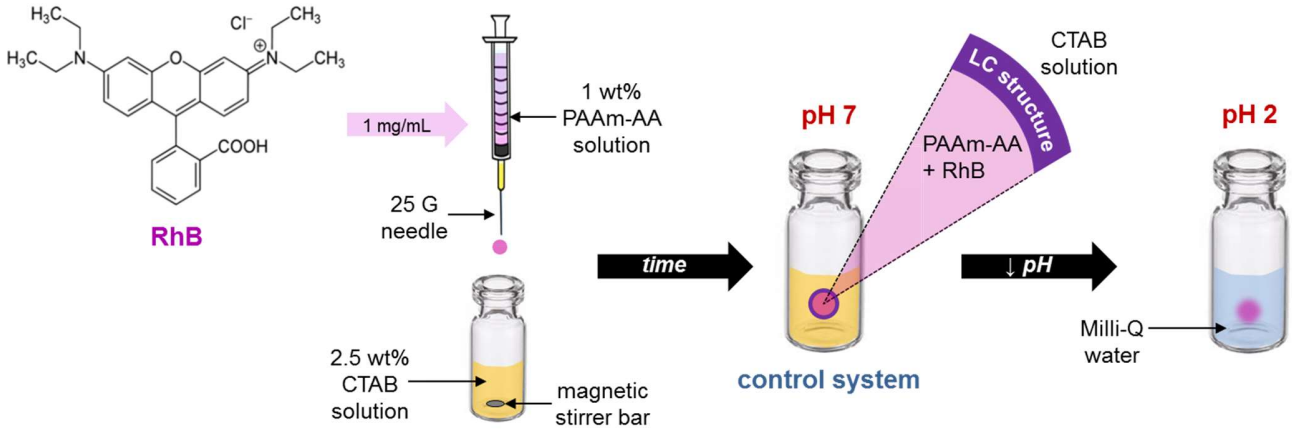
RhB
1 mg/mL
1 wt%
PAAm-AA
solution
25 G
needle
2.5 wt%
CTAB
solution
magnetic
stirrer bar
time
pH 7
LC structure
PAAm-AA
+ RhB
CTAB
solution
control system
↓ pH
pH 2
Milli-Q
water

Figure 5

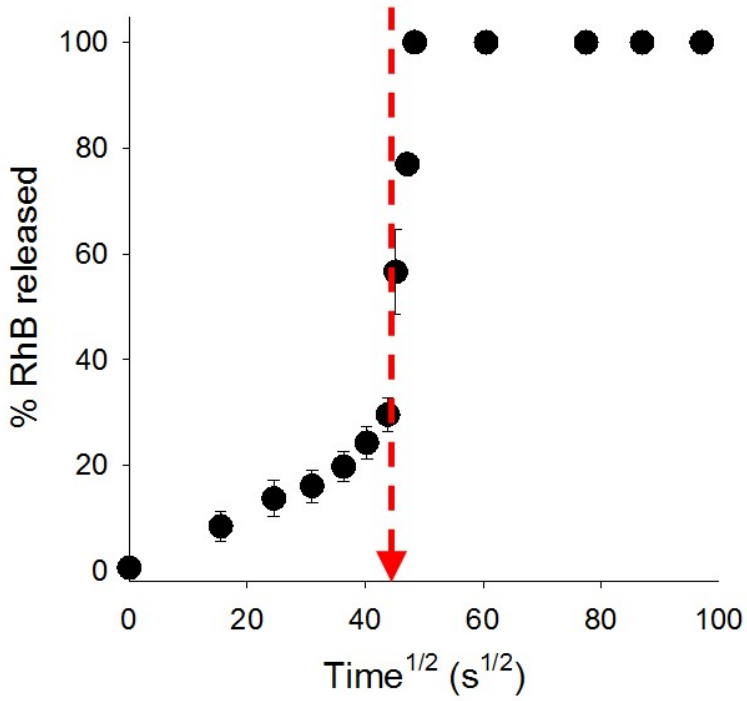

For Table of Contents Only